Journal of Foraminiferal Research, v. 45, no. 2, p. 190–203, April 2015

SHELL DISSOLUTION IN LARGER BENTHIC FORAMINIFERS EXPOSED TO PH AND TEMPERATURE EXTREMES: RESULTS FROM AN IN SITU EXPERIMENT

BRIENNE E. ENGEL[1,2], PAMELA HALLOCK[1,5], ROY E. PRICE[3] AND THOMAS PICHLER[4]

ABSTRACT

Areas where CO_2-enriched gases discharge into shallow-marine environments can serve as natural laboratories to study the effects of elevated pCO_2 (i.e., ocean acidification) on benthic communities. Hydrothermal vents in Tutum Bay, Ambitle Island, Papua New Guinea, occur at depths of ~10 m and are surrounded by a tropical fringing coral reef. Live specimens of seven species of larger benthic foraminifers were collected from a nearby reef location, placed in small mesh bags, and deployed for five days at six different sites along a gradient of temperature (60–29°C) and pH (5.9–8.1). Foraminiferal species that differ in shell structure (porcelaneous vs. hyaline) and composition (high- and intermediate-Mg calcite) were used in the experiment. Approximately 25% of the specimens, representing four of the seven species, retained normal symbiont color and exhibited minimal dissolution when exposed for five days to temperatures up to 60°C and pH as low as 6.2; shells of specimens that lost symbiont color during deployment exhibited extensive corrosion. More than 80% of the specimens, representing at least one of each species, retained normal symbiont color where the temperature was approximately 40°C and pH fluctuated between 5.9 and 7.4. These observations indicate that shells of reef-dwelling foraminifers can substantially resist dissolution, as long as organic matter is largely intact, under pH conditions sufficiently extreme to erase any fossil footprint.

INTRODUCTION

Human activities have increased atmospheric carbon dioxide (CO_2) concentrations from 280 ppmv (pre-industrial) to 400 ppmv (current); this trend is expected to double pre-industrial levels by the end of the century (e.g., Feely et al., 2009; Tans & Keeling, 2013). The CO_2 that the ocean has absorbed since 1950 has resulted in a 0.1 unit decrease in pH of the surface ocean; further decline by as much as 0.3 pH units by the end of the 21st century has been predicted by the Intergovernmental Panel on Climate Change (IPCC, 2013).

Over the past decade, scientists worldwide have become increasingly concerned about the effects of declining pH in surface waters on aquatic biotas, and especially on organisms that produce calcareous shells or skeletons. For example, Kleypas et al. (2006) predicted that by the middle of the century, the increase in the partial pressure of CO_2 (pCO_2) at the sea surface could decrease aragonite saturation in tropical waters by 30% and biogenic aragonite precipitation by 14–30%. While Kleypas et al. anticipated that coral reefs will be particularly vulnerable, other marine ecosystems with common calcifying organisms may be equally at risk (e.g., Cooley et al., 2009, and references therein). Similarly, Gangstø et al. (2008) predicted a decrease in global aragonite production by 29%, calcite production by 13%, and total calcium carbonate ($CaCO_3$) production by 19% by the end of the 21st century.

Hall-Spencer et al. (2008) proposed that shallow-water environments influenced by venting of CO_2-rich gases can provide natural laboratories to study the effects of elevated pCO_2 on benthic communities. That paper and subsequent studies in shallow-water environments off western Italy (Castello Aragonese on the coast of Ischia, Bay of Naples, and Baia di Levante, Vulcano Island, Sicily) have revealed distinct changes in benthic biotas in response to increasing pCO_2 in the water (e.g., Hall-Spencer et al., 2008; Martin et al., 2008; Rodolfo-Metalpa et al., 2010). Some primary producers, notably many diatoms (Johnson et al., 2013) and seagrasses (Russell et al., 2013), increase their rates of primary production with increased pCO_2. Others, especially calcifying macroalgae, can be negatively affected (e.g., Kufner et al., 2008; Campbell & Fourqurean, 2014). Predicted consequences of elevated pCO_2 on benthic communities include major changes in community structure (e.g., Connell et al., 2013, and references therein).

Studies of foraminiferal assemblages, like studies of many other taxa (e.g., Ries et al., 2009), have produced some contrasting results, as summarized in reviews by Keul et al. (2013) and Doo et al. (2014). Mediterranean shallow-water assemblages influenced by low-pH conditions in CO_2 vent fields revealed differences in composition and abundance compared with nearby habitats not influenced by venting (Dias et al., 2010). For example, calcareous foraminiferal species were absent at pH <7.8. Based on similar observations of foraminiferal assemblages in the vicinity of volcanic CO_2 seeps in Milne Bay, Papua New Guinea, Uthicke et al. (2013) predicted high extinction rates in benthic foraminifers by 2100, if ocean acidification proceeds at predicted rates. On the other hand, Pettit et al. (2013) did not find a significant response to reduced pCO_2 in the benthic foraminifers living in somewhat deeper environments in the northern Gulf of California, though they did detect evidence of dissolution in dead shells.

Laboratory experiments examining responses of calcareous foraminifers to elevated pCO_2 and resulting lower pH have also revealed striking differences among taxa (see reviews by Keul et al., 2013; Doo et al., 2014). Among shallow-water taxa, experiments have examined responses of hyaline Rotaliida, including asymbiotic taxa (especially *Ammonia* spp.) and tropical reef-associated taxa, including amphisteginids, calcarinids, and nummulitids, that host algal endosymbionts (e.g., Lee, 2006). Responses to

[1] College of Marine Science, University of South Florida, 830 1st St S., St. Petersburg, FL 33701, USA
[2] Molecular Oncology Program, H. Lee Moffitt Cancer Center and Research Institute, 12902 Magnolia Drive, Tampa, FL 33612, USA
[3] School of Marine and Atmospheric Sciences, SUNY Stony Brook, Stony Brook, NY 11794, USA
[4] FB 5 Geosciences, University of Bremen, Germany
[5] Correspondence author. E-mail: pmuller@usf.edu

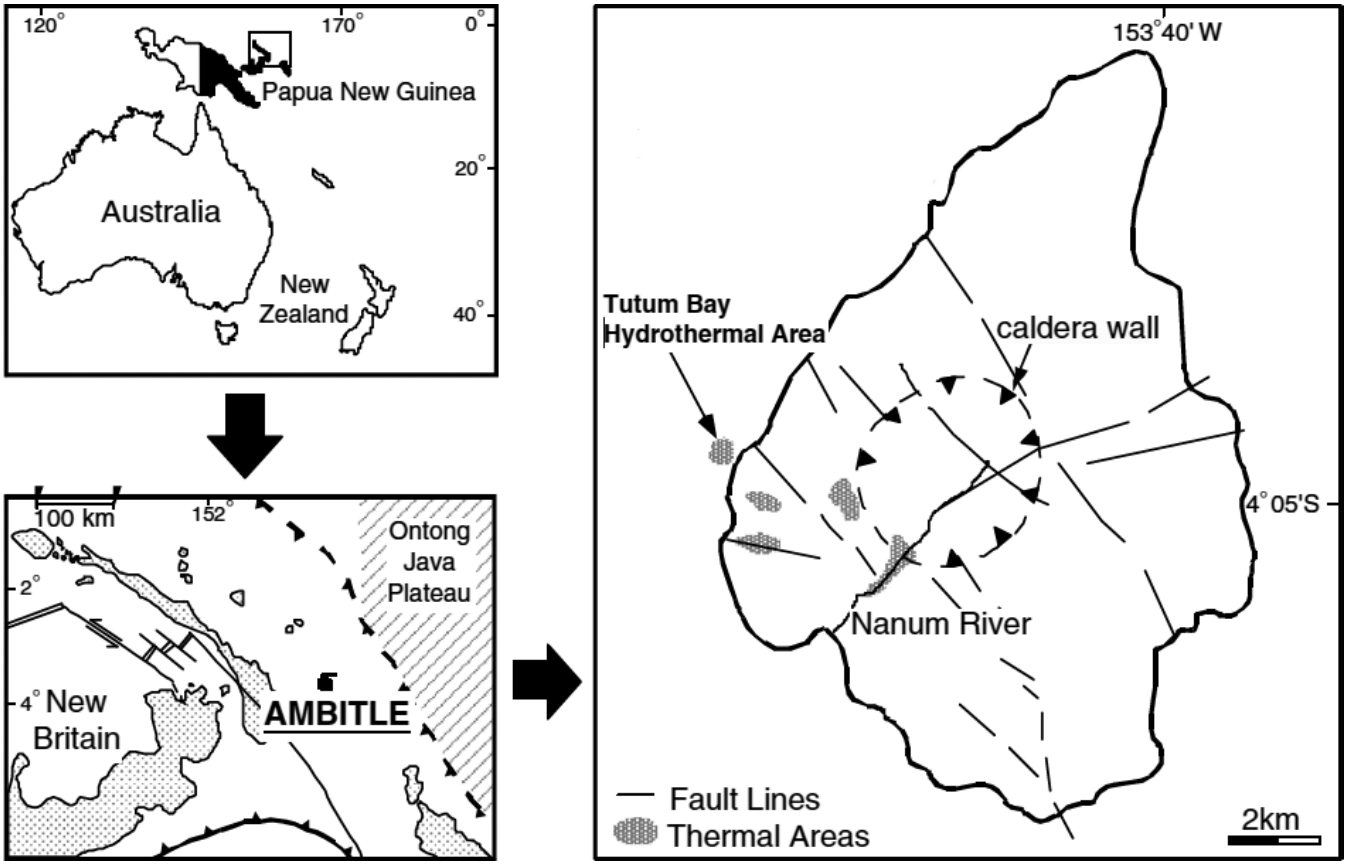

FIGURE 1. Location of Ambitle Island (4°05′S, 153°40′E) and the shallow-water hydrothermal vent system (modified from Price & Pichler, 2005).

elevated pCO_2 among the rotaliids have varied from reduced calcification, especially in taxa that lack algal symbionts (e.g., Allison et al., 2010; Dissard et al., 2010; Haynert et al., 2011), to enhancement of growth and photosynthesis in those with algal symbionts, at least at intermediate pCO_2 levels (e.g., Fujita et al., 2011; Hikami et al., 2011). Among the porcelaneous Miliolida, most experiments have utilized members of the Family Soritidae that host dinoflagellate symbionts. Moreover, most experiments with miliolid taxa found reduced calcification at elevated pCO_2 (e.g., Kuroyanagi et al., 2009; Hikami et al., 2011; Reymond et al., 2013), with the notable exception of the study by Vogel & Uthicke (2012), who reported significant increase in calcification rates up to 1925 ppmv.

Most foraminifers that produce calcified shells precipitate calcite. Because Mg^{2+} readily substitutes for Ca^{2+} in the calcite crystal lattice, many taxa precipitate their shells near equilibrium with seawater, producing what is generally referred to as high-Mg calcite (e.g., the miliolid foraminifers). The proportion of Mg^{2+} in high-Mg calcite shells typically is a function of temperature (e.g., Morse & Mackenzie, 1990) and seawater chemistry (Hardie, 1996). Because Mg^{2+} somewhat disrupts the calcite-crystal lattice, high-Mg calcite (>8 mol%) is both more soluble and structurally weaker than low-Mg calcite (Morse & Mackenzie, 1990). Many calcite-producing foraminifers use energy to concentrate Ca^{2+} in (or to remove Mg^{2+} from) the calcifying fluid (e.g., Bentov et al., 2009; Nehrke et al., 2013), resulting in stronger, less soluble shells. Planktic foraminifers produce low-Mg calcite shells, typically with <1 mol% Mg (e.g., Bender et al., 1975), while some benthic foraminifers produce intermediate-Mg calcite shells with as much as 4–6 mol% Mg (e.g., Segev & Erez, 2006; Raja & Saraswati, 2007).

The Tutum Bay Hydrothermal Vent System

The study site for this experiment was Tutum Bay, off the west side of Ambitle Island, which is one of several Pliocene to Holocene alkaline-arc volcanoes in the Tabar-Feni island arc east of the southern part of New Ireland, Papua New Guinea (Fig. 1). The nearshore zone in the bay is characterized by a well-developed fringing coral reef, interrupted by hydrothermal venting that occurs across a broad area, mostly in waters 5–10-m deep (Pichler & Dix, 1996; Pichler et al., 1999a).

Two types of venting have been described in Tutum Bay, focused and diffuse. Focused discharge of a clear, two-phase fluid occurs at several discrete ports, 10–15 cm in diameter, with an estimated flow rate up to 300–400 L/min (Pichler & Dix, 1996; Pichler et al., 1999b; Price & Pichler, 2005). Temperatures at these ports are typically between 89°C and 98°C. The ports exhibit hydrothermal precipitates, predominantly aragonite and iron oxyhydroxides described as ferrihydrite (Pichler & Veizer, 1999, 2004; Price & Pichler, 2005). Dispersed or diffuse discharge of streaming gas bubbles occurs directly through sandy or pebbly unconsolidated substrate. The gas composition of

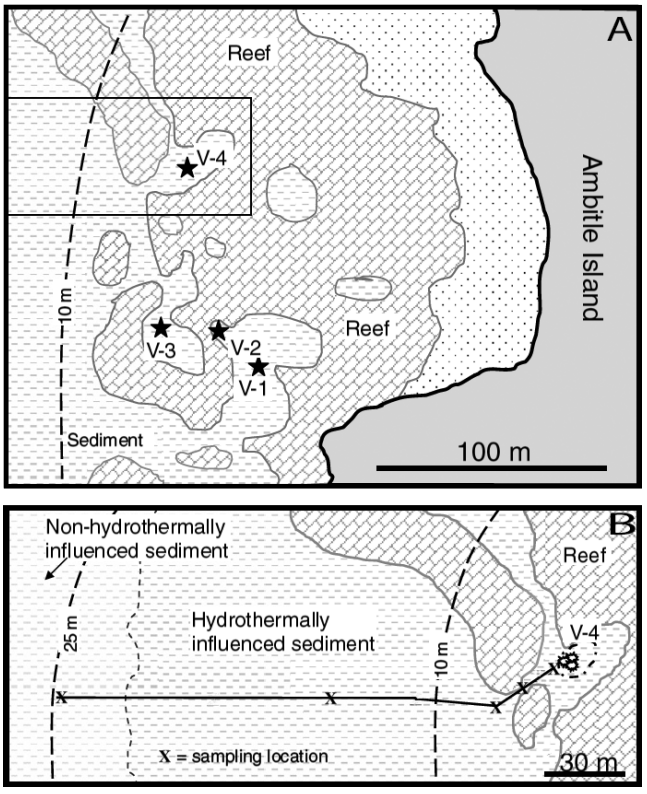

FIGURE 2. **A** Location of Vent 4 (V-4) in relation to Ambitle Island; **B** location of the Vent 4 transect line (modified from Price & Pichler, 2005). Distances from the vent at locations (X) are 7.5 m, 15 m, 30 m, 90 m, and 180 m, respectively. The reference site was located at 10-m depth on reef substrate south of the vent field, outside the area depicted in 2A.

both focused and diffuse discharge varies from 93–98% CO_2, with minor amounts of nitrogen (N_2, 2–5%), methane (CH_4, ≤2%), oxygen (O_2, <1%), and trace amounts of helium. The sediments around the vent sites are coated with ferrihydrite and are derived from the andesitic and dacitic rocks of Ambitle Island (predominantly feldspar, hornblende, pyroxene, and magnetite).

The hydrothermal fluids are predominantly of meteoric origin; vent fluids contain ~10% seawater and are slightly acidic (pH ~6; Pichler et al., 1999a). The vent fluids are substantially enriched in As, Fe, Mn, Cs, Tl, Si, and HCO_3, and slightly enriched in Mg, Zn, Sb, F, Cu, Co, Rb, Ba, Pb, Ni, and Mo relative to ambient seawater, whereas concentrations of Cl, Na, Br, K, SO_4^{2-}, Ca, and Sr are substantially less than in seawater (Pichler et al., 1999a; Pichler, 2005). More detailed descriptions of Tutum Bay hydrothermal vent fluids and precipitates are available elsewhere (e.g., Pichler & Dix, 1996; Pichler et al., 1999a, b; Price & Pichler, 2005; Price, 2008).

The primary focus of field research at the Tutum Bay site in 2003 and 2005 was to determine the influence of arsenic on geochemistry (e.g., Price & Pichler, 2005; Price et al., 2007), microbiology (Akerman et al., 2011; Meyer-Dombard et al., 2012, 2013), benthic invertebrates (Karlen et al., 2010; Price et al., 2013), and benthic foraminiferal assemblages (McCloskey, 2009). However, Pichler et al. (2006) noted the absence of foraminifers and mollusks in

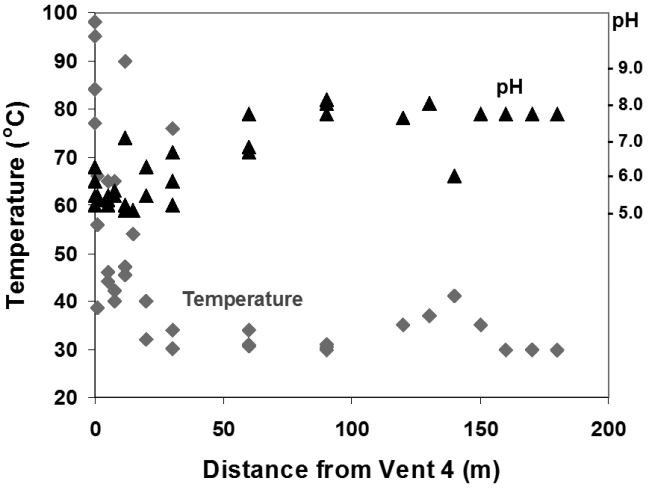

FIGURE 3. Temperature and pH at the sediment-water interface along the transect shown in Fig. 2B with distance from focused venting (from McCloskey, 2009).

sediments near the vents and suggested that temperature or pH might be limiting organisms that produce $CaCO_3$ shells. McCloskey (2009) and Karlen et al. (2010) reported inventories of foraminifers and mollusks, respectively, along a transect extending away from Vent 4 (Fig. 2; described by Pichler et al., 1999a, 2006). Shells of both groups were completely absent in sediments at 7.5 m from the vent, rare at 60 m, and abundant beyond 150 m, indicating that the low pH values associated with the hydrothermal activity played an important role in composition of affected sediments.

The transect from Vent 4 (Fig. 2) was established in 2003, extending from the area of focused venting along a sand channel to the southwest, to an area 225-m distant where the character of the sediment (i.e., color, mineralogy) appeared to be unaffected by hydrothermal activity, as described by Price & Pichler (2005). Temperature and pH of waters recorded at the sediment/water interface along the transect revealed hydrothermal influence extending to 150 m away from the vent site (Fig. 3). Temperatures decreased from 94°C near the vents to consistently ambient seawater (29–31°C) at ~180 m away from the vents. Temperature fluctuated as much as 60°C and pH varied ≥1 unit along the first 30 m of the transect. Beyond 30 m, out to 150 m along the transect, temperature spikes of ≤10°C were recorded. The pH increased from ~6 near the vents to ~8 beyond 150 m.

EXPERIMENTAL RATIONALE AND OBJECTIVES

The experiment described in this paper was prompted by two seemingly contradictory field observations. The first was that changes in the flow path of some hydrothermal vents were accompanied by dissolution of reefal $CaCO_3$. At the same time, despite the extreme environmental conditions in the vent fields, foraminifers were observed alive on rocks that were directly exposed to vent waters in areas devoid of biogenic $CaCO_3$ in the sediments (McCloskey, 2009).

When the research team returned to Tutum Bay in 2005, a small in situ experiment was initiated using larger benthic

TABLE 1. Foraminiferal species used in this experiment, including their higher taxonomy, type of wall structure, and calcite type.

Species	Order	Family	Wall structure	Shell calcite
Amphisorus hemprichii	Miliolida	Soritidae	Porcelaneous	High-Mg
Amphistegina lessonii	Rotaliida	Amphisteginidae	Hyaline	Intermed.-Mg
Amphistegina lobifera	Rotaliida	Amphisteginidae	Hyaline	Intermed.-Mg
Amphistegina radiata	Rotaliida	Amphisteginidae	Hyaline	Intermed.-Mg
Calcarina defrancii	Rotaliida	Calcarinidae	Hyaline	High-Mg
Calcarina gaudichaudii	Rotaliida	Calcarinidae	Hyaline	High-Mg
Heterostegina depressa	Rotaliida	Nummulitidae	Hyaline	High-Mg

foraminifers found abundantly in adjacent reefal environments. The goals were simply to determine where along the temperature gradient specimens might survive limited-duration exposure, and how much shell dissolution might be observed along the pH gradient.

METHODS

Foraminiferal specimens for the experiment were collected at a water depth of ~10 m (similar to the depth at Vent 4) in a nearby coral-dominated area that was not directly affected by hydrothermal venting. At this location, the sediment was predominantly $CaCO_3$ bioclastic debris that included a visible assemblage of larger foraminiferal shells. Live specimens were used to ensure minimal pre-experimental damage to shells, with the expectation that the temperature extremes would quickly kill the experimental specimens at sites influenced by diffuse venting.

Live specimens representing seven species of larger benthic foraminifers were included in this experiment: *Amphisorus hemprichii* Ehrenberg, 1839 (genus subsequently abbreviated *As.*); *Amphistegina lessonii* d'Orbigny, 1826 (genus subsequently abbreviated *Am.*); *Am. lobifera* Larsen, 1976; *Am. radiata* (Fichtel & Moll, 1798); *Calcarina defrancii* d'Orbigny, 1826; *C. gaudichaudii* d'Orbigny, 1840; and *Heterostegina depressa* d'Orbigny, 1826. All occur abundantly in Tutum Bay reef environments; *Am. lessonii and C. defrancii* together make up approximately one third of the foraminiferal assemblage overall (McCloskey, 2009). These seven species represent four different families (Amphisteginidae, Calcarinidae, Nummulitidae, and Soritidae) and include porcelaneous members of the order Miliolida and hyaline members of the order Rotaliida (Table 1).

To collect these specimens, pieces of reef rubble were collected into a zipper-sealed bag and scrubbed with a small brush, a standard method for collecting substantial numbers of live larger foraminifers (e.g., Hallock et al., 1986; Hallock, 2000). The resultant sediment slurry was sieved using a 250-μm mesh to remove finer material, retaining the larger foraminiferal specimens. Specimens selected for the experiment were individually determined to be alive and in near-perfect condition, based on visual inspection and the nearly 40 years of experience that one of us (PH) has had working with live larger foraminifers in both field and laboratory settings. These specimens were individually placed into 13 small, 200-μm mesh pouches (~ 6 × 8 cm). The species used in the experiment were selected because they were sufficiently abundant in the bulk sample to provide at least two specimens for all treatments (Table 2).

The mesh bags were randomly assigned to six experimental treatments, two bags per treatment. Pairs of bags were placed at 7.5 m, 15 m, 30 m, 90 m, and 180 m away from focused venting along the transect described in the Introduction (Fig. 2b). The last pair of bags was placed at the location where the specimens were originally collected (i.e., the reference site). The bags were deployed in contact with the sediment by cable-tying each pair to a scuba weight, along with a StowAway® Tidbit® temperature logger. Water from the sediment-seawater interface at each deployment site was hand collected for pH and salinity measurements by placing air-filled 50 mL HDPE bottles onto the surface sediment and slowly inverting. Samples were brought immediately on board, where pH was measured using a Myron-L Ultrameter™ Model 6P. Shipboard readings were compared with and found to be very similar to those made in situ using a pH meter with an underwater housing (Price, 2008). Salinity was measured using a hand-held refractometer.

To test physicochemical conditions along the transect (Price & Pichler, 2005; Price 2008), 12 pore-water samples were collected from a sediment depth of 10 cm using a Teflon probe connected to a 60 mL syringe. Detailed descriptions of field and laboratory methods can be found elsewhere (Price & Pichler, 2005; Price 2008). Saturation

TABLE 2. Number of specimens of each species by deployment site [distance from vent (m); replicates combined; Ref. = Reference Site].

	7.5 m	15 m	30 m	90 m	180 m	Ref. site	Starting material	Species totals
As. hemprichii	22	23	22	21	20	20	10	**138**
Am. lessonii	5	5	5	5	10	4	2	**36**
Am. lobifera	5	2	2	2	3	2	2	**18**
Am. radiata	6	6	6	6	6	6	3	**39**
C. defrancii	3	13	13	6	5	5	3	**48**
C. gaudichaudii	10	11	10	10	10	10	8	**69**
H. depressa	2	2	2	2	2	2	2	**14**
Site Totals	**53**	**62**	**60**	**52**	**56**	**49**	**30**	**362**

TABLE 3. Summary of descriptions of treatment sites and summary observations of dissolution; temperature, salinity, and pH ranges are based on measurements taken along the same transect as this study and published elsewhere (Price & Pichler, 2005; McCloskey, 2009; Karlen et al., 2010). Ref.= reference site.

	Survival		Environmental conditions and shell descriptions				
Distance from vent	7.5 m	15 m	7.5 m	15 m	30 m	90 m	Reference & 180 m
Temperature (°C)			42–65	34–48	31–32	31–32	30
pH			6.2	5.9–7.4	6.5–7.5	7.5–7.9	7.9–8.2
Salinity			15	33	30	32	34
Amphisorus hemprechii	7 of 22 (32%)	19 of 23 (83%)	Loss of outer layer of shell	Loss of fine detail	Some loss of surface layer of shell	Intact	Intact
Amphistegina lessonii	2 of 5 (40%)	4 of 5 (80%)	Minor dissolution (live) to complete loss of outer layer (dead)	Some dissolution of surface layer	Minor dissolution on some specimens	Intact	Intact
Amphistegina lobifera	0 of 5 (0%)	1 of 2 (50%)	Complete loss of outer layer	Nearly complete loss of surface layer	Moderate dissolution of surface layer	Intact	Intact
Amphistegina radiata	0 of 6 (0%)	5 of 6 (83%)	Complete loss of outer layer	Nearly complete loss of surface layer	Minor dissolution of surface layer	Some minor dissolution	Intact
Calcarina defrancii	1 of 3 (33%)	9 of 13 (69%)	Minor dissolution (live) to complete loss of outer layer (dead)	Moderate dissolution of surface layer	Minor dissolution of surface layer, breakage	Intact	Intact
Calcarina gaudichaudi	3 of 10 (30%)	11 of 11 (100%)	Minor dissolution (live) to complete loss of outer layer (dead)	Moderate dissolution of surface layer	Minor dissolution of surface layer, breakage	Intact	Intact
Heterostegina depressa	0 of 2 (0%)	2 of 2 (100%)	Extensive dissolution and breakage	Minor dissolution of surface layer, breakage	Minor dissolution of surface layer, breakage	Intact	Intact

indices were calculated for calcite and aragonite with the computer code Geochemist's Workbench® using data from Price (2008). Saturation is expressed as the saturation index [(SI) = log (IAP/K_s)], where IAP is the ion activity product and K_s is the solubility constant for either calcite or aragonite. Negative values indicate under saturation and thus the potential for dissolution.

The thirteenth bag with live foraminiferal specimens was not deployed; it was immediately rinsed with distilled water and air dried to provide a sample of the condition of the original specimens. After five days in contact with the sediment, the other 12 bags were recovered, rinsed with distilled water, and air dried. All material was transported to the University of South Florida and maintained in air-conditioned storage until examination.

Each of the foraminifers removed from the mesh bags was examined using a stereomicroscope, cleaned (if necessary) by gently brushing with a fine-tipped artist's brush, identified to species level, and assigned an identifying code. Each specimen was mounted on an aluminum SEM stub coated with conductive carbon tape and digitally photographed at the highest magnification that would allow a view of the entire shell. Those images, revealing presence or absence of symbiont color, were used to evaluate whether individual specimens were likely alive or dead (e.g., Zohary et al., 1980; Hallock, 1984, 2000) when the sample bags were retrieved.

The SEM stubs were placed in a desiccator overnight, then sputter coated with AuPd alloy. Each specimen was imaged with a scanning electron microscope (Hitachi® S 3500N) under 5 KV, size 4 aperture, 35 spot size and a 40-mm working distance for maximal depth of field and surface-texture detail. All specimens were recorded at the highest magnification that could yield an image of the entire shell (i.e., "full-specimen images"). Dissolution of the shell surface layer for each specimen was assessed visually and compared to the full-specimen SEM images from the reference site.

Selected individuals, at least one per species per deployment site, were further examined for alterations to the shell surface under high magnification (600× for *As. hemprichii*, 1000× for all other species). Two individuals were assessed from the site closest to the vent (7.5 m), one showing minimal damage and one with substantial dissolution. Sets of images were assembled for each species to illustrate the state of the shells based upon visual inspection of the different types of images: digital, full-specimen SEM, and high-magnification SEM.

RESULTS

Because relatively few specimens of some species were available for each treatment (Table 2), the results were primarily qualitative. Those results, along with limited quantitative data and ranges of temperature, pH, and salinity recorded at the sediment surface during deployment, are summarized in Table 3. Additional physiochemical data for pore waters from 10-cm depth along the transect, also collected during the experiment (Table 4), revealed that pore waters were undersaturated with respect to both calcite and aragonite well beyond 90 m from the vent.

Approximately 75% of the specimens deployed 7.5 m from the focused vent exhibited loss of symbiont color and

TABLE 4. Physicochemical data for pore water at 10-cm sediment depth along the transect leading away from Vent 4. SI (saturation Index) = log (IAP/Ks).

Sample ID	Distance m	Temp °C	pH	HCO_3^- mg/L	Mg mg/L	Ca mg/L	Na mg/L	Calcite SI	Aragonite SI
vent 4	0	91	6.1	717	130	195	1060	0.1	−0.1
4B05-0	0	70	6.1	327	795	416	6470	−0.6	−0.8
4B05-7.5	7.5	49	6.2	415	593	213	5100	−0.9	−10.6
4B05-12	12	81	6.2	605	187	213	2170	−0.4	−0.6
4B05-20	20	33	5.9	156	1100	372	9340	−17.4	−19.0
4B05-30	30	31	6.3	198	1090	405	10280	−11.2	−12.8
4B05-60	60	34	6.3	224	1066	377	8686	−1.0	−1.2
4B05-90	90	30	7.6	127	1320	408	10400	0.2	0.0
4B05-120	120	32	6.5	171	1245	407	10200	−0.9	−10.7
4B05-140	140	34	6.0	268	1075	371	8820	−13.7	−15.3
4B05-240	240	30	8.0	154	1260	395	10300	0.6	0.4
4B05-300	300	30	7.6	173	1305	413	10600	0.3	0.1

extensive dissolution. In contrast, 80% of the shells from the 15-m site exhibited normal symbiont color and minimal dissolution. In specimens deployed 30 m, 90 m, and 180 m from Vent 4, normal color was consistently retained and few specimens exhibited even minimal dissolution. A selected subset of scanning-electron micrographs are presented in Figures 4–6; the full set of digital color photographs and electron micrographs can be found in Engel (2010).

Amphisorus hemprichii was the only porcelaneous species sufficiently large and abundant to be included in this experiment. Ten specimens were present in the sample that was killed and set aside at the start of the experiment (Table 2). These specimens appeared dark brown in their centers and lighter brown to white around the periphery; the brown color results from the presence of dinoflagellate symbionts within the shell (e.g., Zohary et al., 1980). These specimens, as expected, showed no dissolution features and shells were entirely intact. Specimens placed at the collection (i.e., reference) site (Figs. 4.1a, b), and those deployed 180 m and 90 m from the vent, exhibited no differences from the starting material. Specimens that were visually intact and exhibited normal symbiont color were found in all treatments (Table 3). Specimens placed 30 m away from the vent site showed only minor dissolution such as loss of fine detail and decreased surface topography in high magnification SEM images. Specimens from the 15-m site were mostly intact but exhibited some dissolution and loss of fine surface detail (Figs. 4.2a, b). Of the 22 experimental specimens from the 7.5-m deployment site, all exhibited some dissolution. Nine specimens lacked symbiont color and exhibited extensive dissolution visible at all magnifications (i.e., extensive dissolution of the outer shell layer, exposing the chamberlets; Figs. 4.3a, b), while six exhibited near-normal color and limited dissolution (minimal loss of the outer layer). The other seven specimens were intermediate in color and degree of dissolution.

Two specimens of *H. depressa* were available for each treatment (Table 2). The two specimens that were killed and set aside before the start of the experiment appeared in shades of golden brown from their diatom symbionts and exhibited no dissolution (Table 3). Specimens from the reference site (Figs. 4.4a, b), as well as those from 180 and 90 m along the transect, showed no visible differences from the starting material. Specimens from all treatments other than 7.5 m exhibited normal golden-brown color, though specimens from 30-m and 15-m treatments (Figs. 4.5a, b) exhibited detectable shell dissolution under high magnification. Both specimens from the 7.5-m site were white and exhibited extensive dissolution and shell breakage (Figs. 4.6a, b).

Eleven specimens of two *Calcarina* species were present in the sample that was killed and set aside at the start of the experiment (three *C. defrancii*, eight *C. gaudichaudii*; Table 2). These specimens also were golden brown, the color of the diatom symbionts within each shell, and exhibited no dissolution (Table 3). This was the case for the reference-site specimens (Figs. 5.1a, b, 5.4a, b), and those deployed at 180 and 90 m from the focused vent. Specimens that were visually intact and exhibited normal symbiont color were present in all trials. Some dissolution was evident under high magnification in *C. defrancii* specimens from the 15-m site (Fig. 5.2b), though not at 30 m, and in *C. gaudichaudii* from both the 30- (Table 3) and 15-m (Fig. 5.5b) sites. Of the three *C. defrancii* deployed 7.5 m from the vent, one exhibited normal color and limited dissolution, while two were white and exhibited extensive dissolution (Fig. 5.3b). Of the ten *C. gaudichaudii* at 7.5 m from the vent, three exhibited normal color and limited dissolution (Table 3), one was intermediate in color and dissolution, while six were white and exhibited extensive dissolution (Fig. 5.6b).

Seven specimens of *Amphistegina* spp. were present in the sample that was killed and set aside before the start of the experiment (two *Am. lessonii*, two *Am. lobifera*, three *Am. radiata*; Table 2). All specimens appeared to have normal coloration of shades of golden brown, demonstrating the presence of diatom endosymbionts within the cytoplasm of each shell, with no dissolution (Table 3). This was also the case for the reference-site specimens (Figs. 6.1, 6.4, and 6.7) and those deployed at 180 m and most at 90 m (Table 3). Specimens available from all treatments ranged from 4–10 for *Am. lessonii*, 2–5 for *Am. lobifera*, and six for *Am. radiata* (Table 2). Specimens that were visually intact and exhibited normal symbiont color were present in all treatments except those at the 7.5-m site for *Am. lobifera* and *Am. radiata*, where all were white (Table 3). The *Am. lessonii* specimens deployed at 15 m (Fig. 6.2) were indistinguishable from those from the reference site. Of the

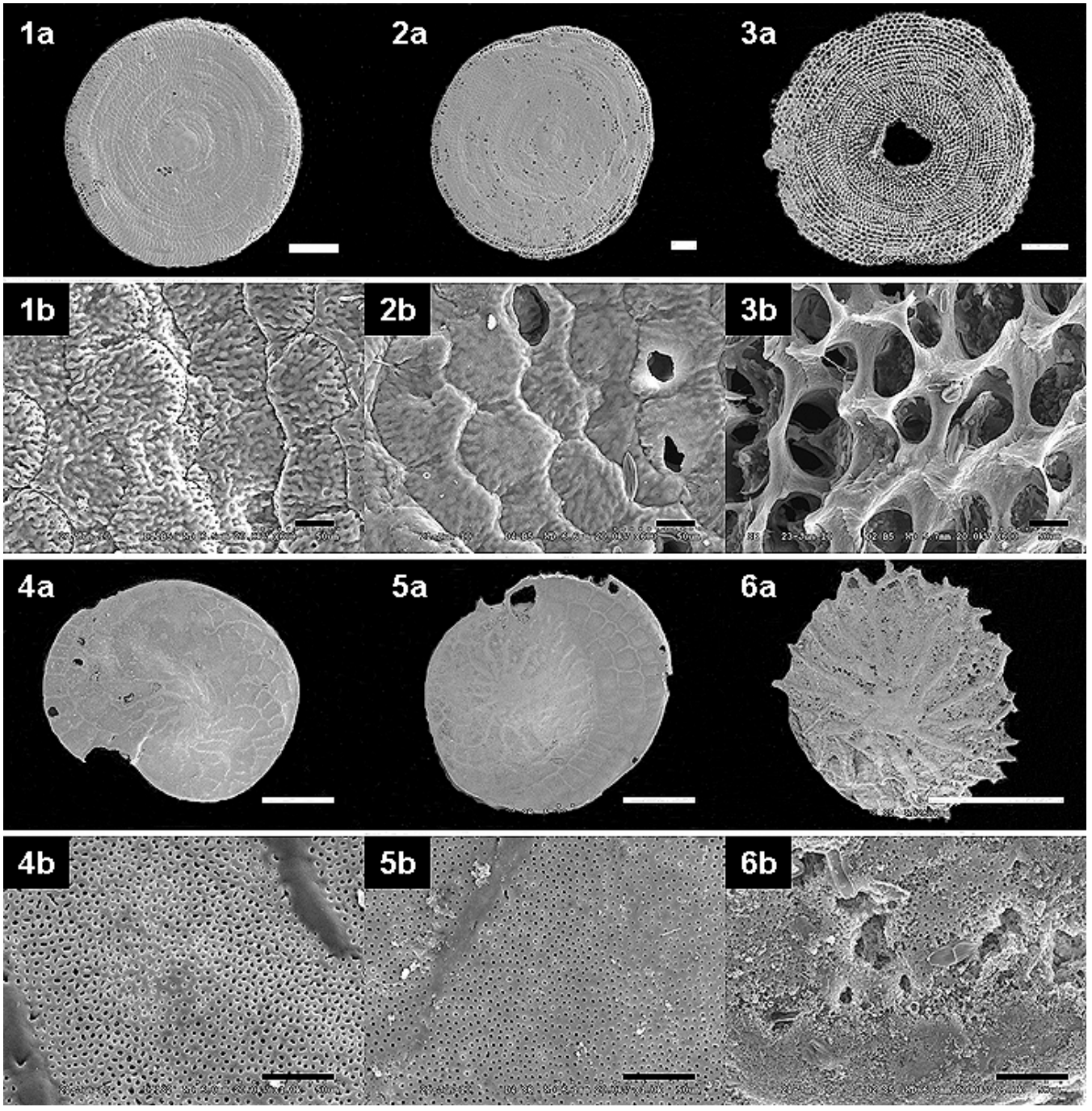

FIGURE 4. **1–3** *Amphisorus hemprichii*: Specimens deployed for five days at reference site (1a, b), 15 m from vent (2a, b), and 7.5 m from vent (3a, b). **4–6** *Heterostegina depressa*: Specimen deployed for five days at Reference site (4a, b), 15 m from vent (5a, b), and 7.5 m from the vent (6a, b). Full-specimen SEMs: scale bar = 0.5 mm; wall surface SEM: scale bar = 25 μm.

five specimens recovered from the 7.5-m site, two retained color and exhibited minimal dissolution, one was intermediate in color and dissolution, and two were white and exhibited extensive dissolution (Figs. 6.3a, b). Results were similar for *Am. lobifera* (Figs. 6.5a, b) and *Am. radiata* (Figs. 6.8a, b) from 15 m. All five of the *Am. lobifera* from 7.5 m exhibited extensive dissolution (Figs. 6.6a, b). Five of the six *Am. radiata* at 7.5 m were white and exhibited extensive dissolution (Figs. 6.9a, b); the other specimen was intermediate in color and degree of dissolution. While specimens of all three species showed reduced dissolution with distance from the vent, *Am. lobifera* and *Am. radiata* exhibited slightly more dissolution than did *Am. lessonii* (Table 3).

DISCUSSION

Effects of Temperature and pH

The completely unexpected observation from this study was the minimal dissolution and retention of normal

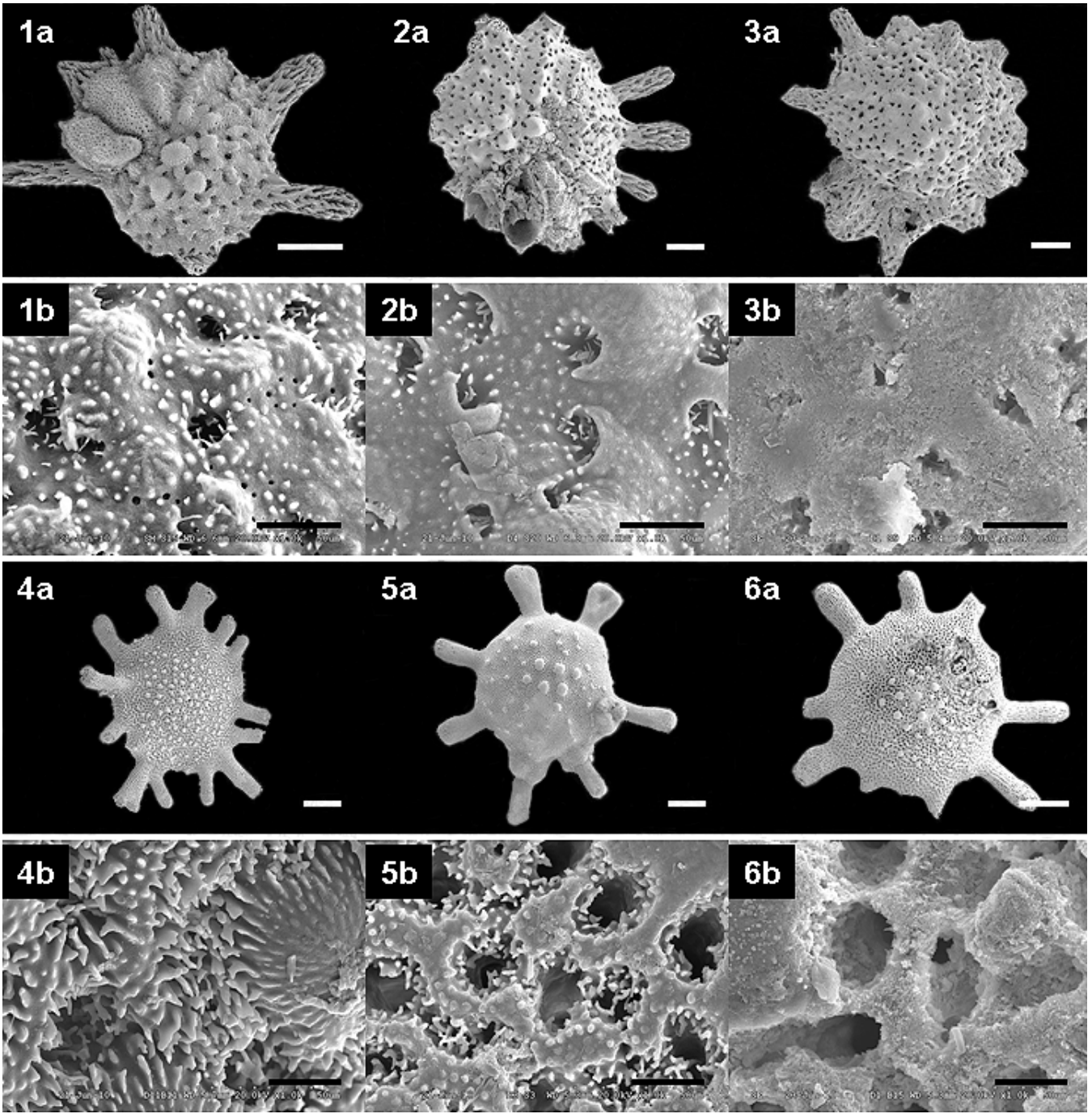

FIGURE 5. **1–3** *Calcarina defrancii*: Specimens deployed for five days at Reference site (1a, b), 15 m from vent (2a, b), and 7.5 m from vent (3a, b); full-specimen SEMs: scale bar = 0.1 mm; wall surface SEM: scale bar = 25 μm. **4–6** *C. gaudichaudi*: Specimen deployed for five days at Reference site (4a, b), 15 m from vent (5a, b), and 7.5 m from the vent (6a, b); full-specimen SEMs: scale bar = 0.5 mm; wall surface SEM: scale bar = 25 μm.

coloration of some individuals, after five days in the extreme conditions resulting from diffuse venting at 7.5 m from the vent. The sediment at this site was consistently uncomfortably warm for researchers. Yet some specimens of four of the species included in the experiment retained the normal color of live specimens and exhibited minimal dissolution. Only specimens that became white during the exposure period exhibited extensive dissolution. Most experimental specimens deployed 15 m from the vent and exposed to diffuse venting retained normal color and exhibited fairly limited dissolution, though this group exhibited the interspecific trends in susceptibility that were more evident in the 7.5-m treatment.

Data collected in 2003 (e.g., Price & Pichler, 2005) indicated that temperatures fluctuated as much as 40°C at 5-cm depth within the sediments along the first 20 m of the transect, while fluctuations of ≥10°C were recorded from 20–100 m from the vent (Fig. 3). Pore-water samples from

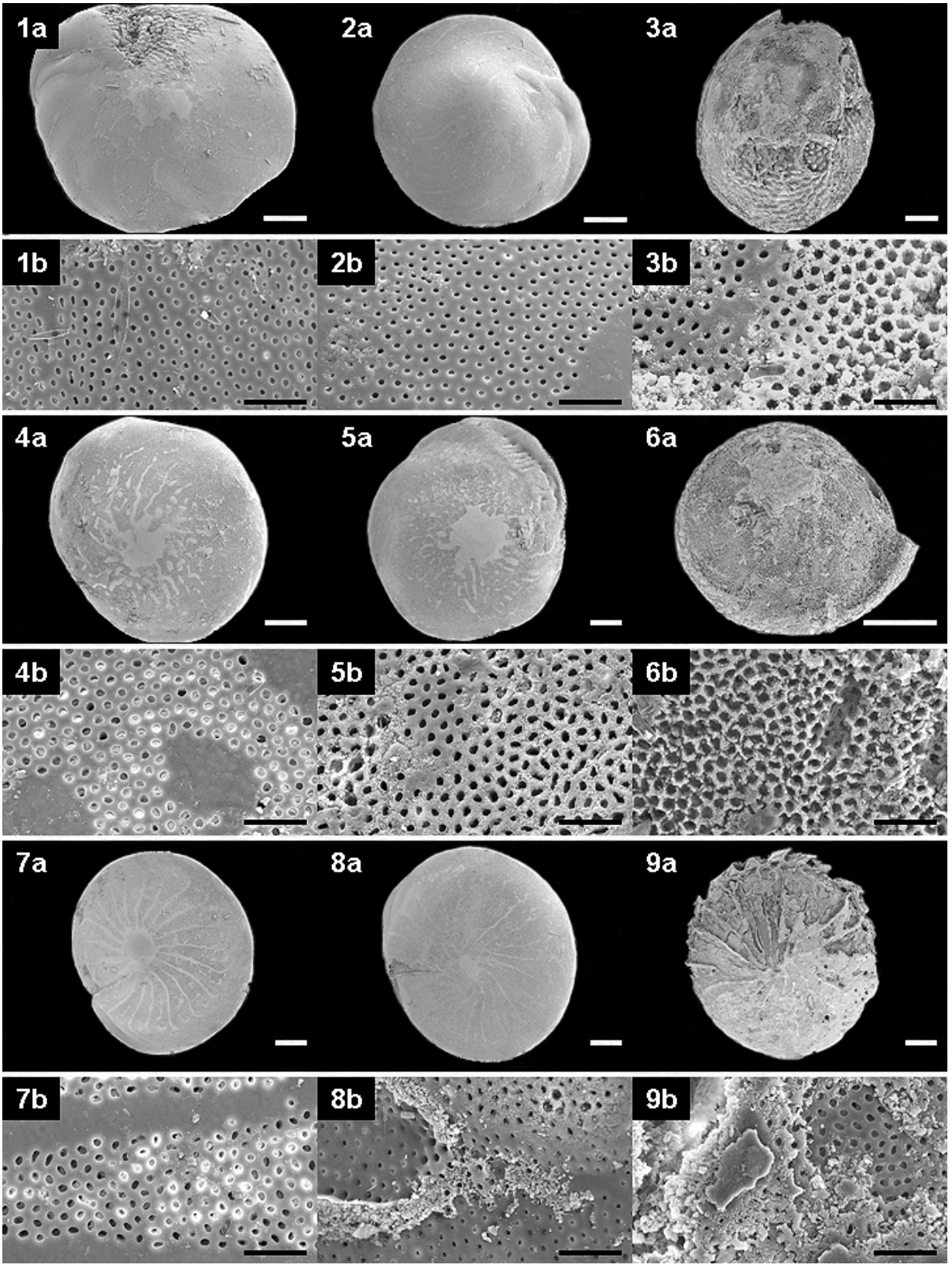

FIGURE 6. **1–3** *Amphistegina lessonii*: Specimens deployed for five days at Reference site (1a, b), 15 m from vent (2a, b), and 7.5 m from vent (3a, b). **4–6** *Am. lobifera*: Specimen deployed for five days at Reference site (4a, b), 15 m from vent (5a, b), and 7.5 m from the vent (6a, b). **7–9** *Am. radiata:* Specimens deployed for five days at Reference site (7a, b), 15 m from vent (8a, b), and 7.5 m from vent (9a, b). Full-specimen SEMs: scale bar = 0.25 mm; wall surface SEM: scale bar = 25 μm.

10-cm depth along the same transect in 2005 (Table 4) were consistent with the results from 2003. Moreover, measurements of pH and temperature sensors deployed with the experimental specimens in 2005 (McCloskey, 2009) were comparable to the measurements taken within the sediments in 2003 and 2005, confirming that experimental specimens were exposed to elevated temperatures and consistently low pH (<7.5) at the 7.5-m, 15-m and 30-m sites (Table 3).

Previous experimental studies suggested an upper temperature limit of about 32°C for many species of larger foraminifers (e.g., Talge & Hallock, 2003; Schmidt et al., 2011; Sinutok et al., 2011; Doo et al., 2014). However, Fujita et al. (2014) reported short-term tolerance of temperatures as high as 40°C. Based on our observations and those of Fujita et al. (2014), a reasonable hypothesis is that some foraminifers can tolerate intermittent temperature extremes as long as repair mechanisms can be activated between pulses of hot water.

The pH of the interstitial fluids increased from ~6 near the vents to 8.1 along the transect, with below-ambient pH and substantial fluctuations observed as far as 150 m from focused venting (Fig. 3; Tables 3, 4). Moreover, the sediments at all of the deployment sites except 180 m and the reference site were essentially devoid of $CaCO_3$ (<1%; Price & Pichler, 2005; Karlen et al., 2010). Saturation indices revealed that calcite and aragonite were consistently undersaturated within the sediments that contained minimal $CaCO_3$, and that pH together with bicarbonate (HCO_3^-) played a major role controlling saturation.

Only the foraminiferal specimens that clearly had died during the exposure experiment, as indicated by color loss, exhibited extensive dissolution. These observations suggest that these foraminifers can survive pH conditions under which their shells have no preservation potential. The amazing potential for survival of some species was also observed by the research team in the field, where foraminifers (especially *C. defrancii*, but also *Am. lessonii* and even small miliolids) were observed living in algal-microbial films exposed directly to vent fluids on volcanic rocks that were noticeably hot to the touch.

The porcelaneous shell structure is three-layered, high-Mg calcite, which forms imperforate, non-lamellar walls. In soritid foraminifers that host algal symbionts, only the characteristically smooth outer layer of calcite crystals extends over individual chamberlets, which allows light to reach the algal symbionts inside (e.g., Cottey & Hallock, 1988). When that outer layer dissolves away, the chamberlets are exposed. In *As. hemprichii*, the only porcelaneous species in the study, dissolution ranged from minor loss of the outer shell layer to loss of the entire center of some specimens deployed 7.5 m from the vent. Higher magnification SEM images revealed loss of fine detail and decreased surface topography at deployment distances up to 30 m from the vent. Despite notable dissolution, nearly a third of the specimens retained normal symbiont color when deployed for five days at the 7.5-m site. Several previous studies have reported dissolution in *Archaias angulatus* (Fichtel & Moll) that were collected alive (Macintyre & Reid, 1998; Crevison & Hallock, 2007; Souder et al., 2010), thus, tolerance to some dissolution may be common in this group. Unlike the rotaliid foraminifers, miliolids do not precipitate new laminae over the entire shell with each chamber addition (e.g., Erez, 2003), and apparently are unable to repair damage to the shell surface.

The hyaline calcareous representatives have a perforate, laminar wall structure composed of oriented calcite crystals. In contrast to the porcelaneous foraminifers, the hyaline taxa examined deposit a new layer of calcite over the shell with each chamber addition, allowing repair of damage to the shell surface. The calcarinids and nummulitids produce high-Mg calcite in the 11–13 mole% range, while *Amphistegina* spp. produce intermediate-Mg calcite shells, commonly ~4–5 mole% Mg (Segev & Erez, 2006; Raja & Saraswati, 2007; Engel, 2010).

Specimens of *H. depressa* are inherently fragile, making it difficult to determine how much of the breakage was due to dissolution and how much was caused by handling. Nonetheless, extensive dissolution occurred in the specimens deployed at the 7.5-m site. Unfortunately, the few specimens available for the experiment (2/site) limited interpretation. Nevertheless, observations for *H. depressa* are comparable to those of the other species.

At lower magnifications, the two *Calcarina* species appeared to be the least affected by hydrothermal venting. However, when examined by SEM at higher magnification, the loss of fine detail, such as the needle-like projections on the shell surface and in the pores, revealed some degree of dissolution, especially in *C. gaudichaudii*. Some fine detail was lost on *C. defrancii* specimens deployed 15 m from the vent, while *C. gaudichaudii* specimens lost fine detail out to 30 m from the vent (Table 3). The extensive surface area provided by the very complex texture of *Calcarina* spp. may enhance susceptibility to dissolution. Khanna et al. (2013) similarly found fine-scale dissolution of ornamentation of *Haynesina germanica* (Ehrenberg) at high pCO_2, concluding that loss of structures important to feeding would reduce the fitness of such individuals.

Differences among the three *Amphistegina* species indicated that sensitivity to heat stress and acidity may be species specific. All experimental specimens of *Am. lobifera* and *Am. radiata*, along with *H. depressa*, lost all symbiont color and exhibited extensive dissolution after five days at the 7.5-m site. In contrast, some *Am. lessonii* specimens retained normal color at the same site, and those specimens exhibited minimal dissolution. *Amphistegina lobifera* and *Am. radiata* also exhibited some breakage and surficial dissolution in specimens deployed as much as 90 m from the vent (Table 3). Such interspecific differences in susceptibility to dissolution among *Amphistegina* spp., as well as between the *Calcarina* spp., could be an interesting direction for future research utilizing molecular biomarkers (e.g., Prazeres et al., 2011, 2012).

Elevated temperature was the most likely source of mortality over the short length of the experiment. Foraminiferal shells of specimens that retained normal symbiont color substantially resisted dissolution, while those that exhibited extensive dissolution were white. Unfortunately, logistical limitations prevented examination of experimental specimens in the field immediately upon recovery. However, symbiont color in specimens killed

quickly and dried is a more reliable indicator of whether specimens were alive when collected (e.g., Zohary et al., 1980; Hallock et al., 1986) than rose Bengal dissolved in ethanol, because ethanol leaches symbiont color (Hallock, 2000).

Shell structure appeared to be a better predictor of susceptibility to dissolution than shell chemistry; dissolution was most extensive in the porcelaneous *As. hemprichii* and the relatively delicate *H. depressa*, both of which produce high-Mg calcite shells. Among the *Amphistegina* and *Calcarina*, differences appeared to be more closely related to interspecific differences in mortality than in differences between intermediate- and high-Mg calcite. A plausible explanation may simply be that the water chemistry was sufficiently acidic that, once the foraminifer died, dissolution proceeded rapidly regardless of shell chemistry.

Our observations from hydrothermal venting may appear to be in sharp contrast with results from ambient-temperature CO_2-seeps in the Mediterranean Sea (e.g., Dias et al., 2010), where calcareous foraminifers are absent at pH $\leq$7.6. The effects of such seeps on foraminifers in Milne Bay, Papua New Guinea, reported by Uthicke et al. (2013), are quite similar to those from the Mediterranean. However, the differences are not as problematic as they first appear. The Milne Bay samples were reported to be surficial sediments (Uthicke et al., 2013) and the decline in density and diversity of foraminiferal shells in those samples corresponds to a decrease in $CaCO_3$ in the sediments to $<$1% at a pH of $\sim$7.8. The sediments along the Tutum Bay transect also were essentially devoid of $CaCO_3$ out to 150 m, where the pH was $<$7.8. Thus, although live foraminifers showed little or no dissolution beyond 30 m from the vent, the shells did not preserve in the sediment. Moreover, most reef-dwelling foraminifers do not live in sediments, but rather on firm substrates such as reef rock and marine plants (e.g., Martin, 1986; Hallock, 2012). On such substrata, live foraminifers were found just centimeters away from focused venting (McCloskey, 2009).

Several studies have reported observations that reflect differences between survival and preservation potential. Uthicke et al. (2013) noted that *Am. lessonii* and two species of *Elphidium* increased in relative importance in sediments at intermediate pCO_2 and a pH of $\sim$7.8, but observed corrosion and pitting of the shells. McIntyre-Wressnig et al. (2013) reported pitting in shells in experimental studies of *Am. gibbosa* exposed in culture to 2000 ppmv pCO_2 for six weeks, while finding that neither survival nor cellular energy levels were affected. McIntyre-Wressnig et al. (2014) similarly found that two common temperate benthic species showed no direct effect of high pCO_2 on survival or fitness even when seawater was undersaturated with respect to calcite.

Implications: Past and Future

In the middle of the 20th century, Newell (e.g., 1962, 1982) recognized that mass extinction events in the fossil record are characterized by widespread $CaCO_3$-depositional hiatuses, marked by loss of high proportions of $CaCO_3$-producing, reef-associated organisms (e.g., Kiessling et al., 2008; Greene et al., 2012, and references therein). If atmospheric pCO_2 increases and oceanic pH declines, as predicted through this century and beyond (e.g., Feely et al., 2009; IPCC, 2013), the Anthropocene mass extinction event (e.g., Saxon, 2008) will also be characterized by $CaCO_3$-poor marine sediments (e.g., Hallock, 1996, 2005). Increasing rates of extinctions are predicted for calcifying organisms under increasing atmospheric and ocean pCO_2 concentrations, based on a range of studies and methods, including observations at ambient-temperature CO_2 seeps (e.g., Dias et al., 2010; Uthicke et al., 2013).

Nevertheless, there are clearly species-specific differences in the vulnerability of benthic foraminifers (e.g., McIntyre-Wressnig et al., 2014). The geologic record indicates that some species of larger foraminifers will likely survive ocean acidification. The nearly circumtropical distributions and long fossil records of *Amphistegina*, *Heterostegina*, and the Soritidae, along with their ability to survive in suitable microenvironments, suggest their potential to be future ''Lazarus taxa'' (Flessa & Jablonski, 1983), which disappear from the sedimentary record for extended times, not because they become extinct but because ocean chemistry prevents preservation and fossilization of their shells.

Environments with limestone substrata that are within the euphotic zone may continue to support larger benthic foraminiferal populations, even as atmospheric CO_2 increases. Precipitation of shells is enhanced by photosynthesis during daylight hours. Our experiment, as well as those of Dissard et al. (2010), McIntyre-Wressnig et al. (2014), and others, indicates that, once precipitated, shell calcite is relatively protected from dissolution while the foraminifer is alive. While lower pH conditions will require greater energy expenditure to precipitate $CaCO_3$, photosynthesis by diatom symbionts may be enhanced by higher pCO_2 (e.g., Johnson et al., 2013). The enhancement of photosynthesis of their diatom symbionts may help explain why diatom-bearing taxa exhibit minimal impairment, or even enhancement of growth, when cultured under elevated pCO_2 (McIntyre-Wressnig et al., 2013; Doo et al. 2014).

Larger benthic foraminifers diversified and were major $CaCO_3$ producers in the Paleogene, when global temperatures and atmospheric pCO_2 levels were at least as high as predicted for the end of this century. Under future atmospheric CO_2 concentrations, terrestrial weathering processes and dissolution of marine carbonates eventually will restore carbonate saturation of the surface oceans to levels that no longer dissolve $CaCO_3$ shells and skeletons (e.g., Kump et al., 2009). Under such saturation states, larger benthic foraminifers might again dominate shelf carbonate factories. The short experiment reported here cannot refute predictions of future extinctions of larger benthic foraminifers (e.g., Uthicke et al., 2013). Nevertheless, our results, in the context of other studies, indicate substantial resiliency of some taxa. Considered in the larger context of their widespread distributions and the roughly 50–60 million-year fossil record of families such as the Amphisteginidae and Nummulitidae (e.g., Hallock, 1985), one can speculate that at least some larger foraminiferal taxa should survive ocean acidification, even if their shells do not.

SUMMARY

1. Individual specimens of four out of seven larger benthic foraminiferal species retained normal symbiont color and thus appeared to survive exposure to temperature fluctuations of up to 60°C and pH as low as 6.2 for five days; individuals of all seven species appeared to survive exposure to 40°C and pH fluctuations from 5.9–7.4.
2. Elevated temperature was the likely source of mortality in specimens that lost all symbiont color, indicating death during the experiment.
3. Specimens that retained normal symbiont color exhibited only limited dissolution; specimens that lost most or all symbiont color exhibited extensive dissolution.
4. Shell structure was a better predictor of susceptibility to dissolution than shell chemistry:
    a. Dissolution was most extensive in the porcelaneous *Amphisorus hemprichii*, which produce nonlamellar, high-Mg calcite shells.
    b. Among the hyaline species, the fragile, high Mg-calcite shells of *Heterostegina depressa* exhibited the most dissolution, while minimal differences were observed between high-Mg calcite *Calcarina* spp. and intermediate-Mg calcite *Amphistegina* spp.
5. Species-specific differences were evident: *Amphistegina lessonii* appeared to survive the environmental extremes longer than *Am. lobifera* and *Am. radiata*, while more *Calcarina defrancii* appeared to survive and exhibited less dissolution than *C. gaudichaudii*.
6. All seven species survived short-term exposure to physicochemical conditions under which their dead shells would dissolve and not produce a fossil footprint.

ACKNOWLEDGMENTS

We thank Dr. E. S. VanVleet and the late Dr. Benjamin Flower for reading early drafts, Tony Greco for expert advice on the use of the SEM, and Drs. Willem Renema and Johann Hohenegger for assistance with *Calcarina* spp. identification. Professor Dr. Malcolm Hart, Assistant Editor Rebekah Baker, and two anonymous reviewers provided comments that improved the manuscript. Financial support for the collection trip came from the National Science Foundation (grant BE: CBC# 0221834) awarded to Thomas Pichler and others. Impetus for the microscopic analyses came during collaboration with J. M. Bernhard and colleagues, funded by NSF grant OCE-0725966 to J. M. Bernhard and D. C. McCorkle. Financial support for B. Engel came from the USF Presidential Fellowship and the Anne and Werner Von Rosenstiel Endowed Fellowship. This manuscript was submitted, reviewed, revised and accepted for publication during the term of past JFR Editor Paul Brenckle, whom we thank for his efforts. Co-author Dr. Pamela Hallock, now serving as Editor of the Journal of Foraminiferal Research, was not involved in editing this paper.

REFERENCES

Akerman, N. H., Price, R. E., Pichler, T., and Amend, J. P., 2011, Energy sources for chemolithotrophs in an arsenic- and iron-rich shallow-sea hydrothermal system: Geobiology, v. 9, p. 436–445.

Allison, N., Austin, W., Paterson, D., and Austin, H., 2010, Culture studies of the benthic foraminifera *Elphidium williamsoni*: evaluating pH, [CO_3^{2-}] and inter-individual effects on test Mg/Ca: Chemical Geology, v. 275, p. 87–93.

Bender, M. M., Lorens, R. B., and Williams, D. F., 1975, Sodium, magnesium and strontium in the tests of planktonic foraminifera: Micropaleontology, v. 21, p. 448–459.

Bentov, S., Brownlee, C., and Erez, J., 2009, The role of seawater endocytosis in the biomineralization process in calcareous foraminifera: Proceedings of the National Academy of Sciences, v. 106, p. 21,500–21,504.

Campbell, J. E., and Fourqurean, J. W., 2014, Ocean acidification outweighs nutrient effects in structuring seagrass epiphyte communities: Journal of Ecology, v. 102, p. 730–737.

Connell, S. D., Kroeker, K. J., Fabricius, K. E., Kline, D., and Russell, B. D., 2013, The other ocean acidification problem: CO_2 as a resource among competitors for ecosystem dominance: Philosophical Transactions of the Royal Society B, Biological Sciences, v. 368, 20120442.

Cooley, S. R., Kite-Powell, H. L., and Doney, S. C., 2009, Ocean acidification's potential to alter global marine ecosystem services: Oceanography, v. 22, p. 172–181.

Cottey, T. L., and Hallock, P., 1988, Test surface degradation in *Archaias angulatus*: Journal of Foraminiferal Research, v. 18, p. 187–202.

Crevison, H., and Hallock, P., 2007, Anomalous features observed on tests of live Archaiasine foraminifers from the Florida Keys, USA: Journal of Foraminiferal Research, v. 37, p. 223–233.

Dias, B. B., Hart, M. B., Smart, C. W., and Hall-Spencer, J. M., 2010, Modern seawater acidification: the response of foraminifers to high-CO_2 conditions in the Mediterranean Sea: Journal of the Geological Society of London, v. 167, p. 843–846.

Dissard, D., Nehrke, G., Reichart, G. J., and Bijma, J., 2010, Impact of seawater pCO_2 on calcification and Mg/Ca and Sr/Ca ratios in benthic foraminifera calcite: results from culturing experiments with *Ammonia tepida*: Biogeosciences, v. 7, p. 81–93.

Doo, S. S., Fujita, K., Byrne, M., and Uthicke, S., 2014, Fate of calcifying tropical symbiont-bearing large benthic foraminifera: living sands in a changing ocean: Biological Bulletin, v. 226, p. 169–186.

Engel, B., 2010, Effects of a shallow-water hydrothermal vent gradient on benthic calcifiers, Tutum Bay, Ambitle Island, Papua New Guinea: University of South Florida Graduate School Theses and Dissertations, http://scholarcommons.usf.edu/etd/3553.

Erez, J., 2003, The source of ions for biomineralization in foraminifera and their implications for paleoceanographic proxies, *in* Dove, P. M., et al. (eds.), Biomineralization: Mineralogical Society of America, v. 54, p. 115–149.

Feely, R. A., Doney, S. C., and Cooley, S. R., 2009, Ocean acidification: present conditions and future changes in a high-CO_2 world: Oceanography, v. 22, p. 39–47.

Flessa, K. W., and Jablonski, D., 1983, Extinction is here to stay: Paleobiology, v. 9, p. 315–321.

Fujita, K., Hikami, M., Suzuki, A., Kuroyanagi, A., Sakai, K., Kawahata, H., and Nojiri, Y., 2011, Effects of ocean acidification on calcification of symbiont-bearing reef foraminifers: Biogeosciences, v. 8, p. 2089–2098.

Fujita, K., Okai, T., and Hosono, T., 2014, Oxygen metabolic responses of three species of large benthic foraminifers with algal symbionts to temperature stress: PLoS ONE, v. 9, e90304.

Gangstø, R., Gehlen, M., Schneider, B., Bopp, L., Aumont, O., and Joos, F., 2008, Modeling the marine aragonite cycle: changes under rising carbon dioxide and its role in shallow water $CaCO_3$ dissolution: Biogeosciences, v. 5, p. 1057–1072.

Greene, S. E., Martindale, R. C., Ritterbush, K. A., Bottjer, D. J., Corsetti, F. A., and Berelson, W. M., 2012, Recognising ocean acidification in deep time: an evaluation of the evidence for acidification across the Triassic-Jurassic boundary: Earth-Science Reviews, v. 113, p. 72–93.

Hallock, P., 1984, Distribution of selected species of living algal symbiont-bearing foraminifera on two Pacific coral reefs: Journal of Foraminiferal Research, v. 14, p. 250–261.

Hallock, P., 1985, Future farmers of the sea: Natural History, v. 94, p. 60–67.

Hallock, P., 1996, Reefs and reef limestones in earth history, *in* Birkeland, C. (ed.), Life and Death of Coral Reefs: Chapman-Hall Science, New York, p. 13–42.

Hallock, P., 2000, Larger foraminifers as indicators of coral-reef vitality, *in* Martin, R. (ed.), Environmental Micropaleontology: Kluwer Academic/Plenum Publishers, New York, v. 17, p. 121–150.

Hallock, P., 2005, Global change and modern coral reefs: new opportunities to understand shallow-water carbonate depositional processes: Sedimentary Geology, v. 175, p. 19–33.

Hallock, P., 2012, The FORAM Index revisited: usefulness, challenges and limitations: Proceedings of the International Coral Reef Symposium, Cairns, Australia, http://www.icrs2012.com/proceedings/manuscripts/ICRS2012_15F_2.pdf

Hallock, P., Cottey, T. L., Forward, L. B., and Halas, J., 1986, Population dynamics and sediment production by *Archaias angulatus* (Foraminiferida) in Largo Sound, Florida: Journal of Foraminiferal Research, v. 16, p. 1–18.

Hall-Spencer, J. M., Rodolfo-Metalpa, R., Martin, S., Ransome, E., Fine, M., Turner, S. M., Rowley, S. J., Tedesco, D., and Buia, M., 2008, Volcanic carbon dioxide vents show ecosystem effects of ocean acidification: Nature, v. 454, p. 96–99.

Hardie, L. A., 1996, Secular variation in seawater chemistry: an explanation for the coupled secular variation in the mineralogies of marine limestones and potash evaporites over the past 600 my: Geology, v. 24, p. 279–283.

Haynert, K., Schönfeld, J., Riebesell, U., and Polovodova, I., 2011, Biometry and dissolution features of the benthic foraminifer *Ammonia aomoriensis* at high pCO_2: Marine Ecology Progress Series, v. 432, p. 53–67.

Hikami, M., Ushie, H., Irie, T., Fujita, K., Kuroyanagi, A., Sakai, K., Nojiri, Y., Suzuki, A., and Kawahata, H., 2011, Contrasting calcification responses to ocean acidification between two reef foraminifers harboring different algal symbionts: Geophysical Research Letters, v. 38, L19601.

IPCC, Climate Change 2013: the physical science basis, *in* Stocker, T. F., et al. (eds.), Contribution of Working Group I to the Fifth Assessment Report of the Intergovernmental Panel on Climate Change: Cambridge University Press, Cambridge and New York, p. 1–1535.

Johnson, V. R., Brownlee, C., Rickaby, R. E. M., Graziano, M., Milazzo, M., and Hall-Spencer, J. M., 2013, Responses of marine benthic microalgae to elevated CO_2: Marine Biology, v. 160, p. 1813–1824.

Karlen, D. J., Price, R. E., Pichler, T., and Garey, J. R., 2010, Changes in benthic macrofauna associated with a shallow-water hydrothermal vent gradient in Papua New Guinea: Pacific Science, v. 64, p. 391–404.

Keul, N., Langer, G., de Nooijer, L. J., and Bijma, J., 2013, Effect of ocean acidification on the benthic foraminifera *Ammonia* sp. is caused by a decrease in carbonate ion concentration: Biogeosciences, v. 10, p. 6185–6198.

Khanna, N., Godbold, J. A., Austin, W. E. N., and Paterson, D. M., 2013, The impact of ocean acidification on the functional morphology of Foraminifera: PLoS ONE, v. 8, p. e83118.

Kiessling, W., Aberhan, M., and Villier, L., 2008, Phanerozoic trends in skeletal mineralogy driven by mass extinctions: Nature Geoscience, v. 1, p. 527–530.

Kleypas, J. A., Feely, R. A., Fabry, V. J., Langdon, C., Sabine, C. L., and Robbins, L. L., 2006, Impacts of Ocean Acidification on Coral Reefs and Other Marine Calcifiers. A Guide for Future Research: report of a workshop held 18–20 April 2005, St. Petersburg, FL, sponsored by NSF, NOAA, and the U.S. Geological Survey, 88 pp. http://www.ucar.edu/communications/Final_acidification.pdf.

Kuffner, I. B., Andersson, A. J., Jokiel, P. L., Rodgers, K. S., and Mackenzie, F. T., 2008, Decreased abundance of crustose coralline algae due to ocean acidification: Nature Geoscience, v. 1, p. 114–117.

Kump, L. R., Bralower, T. J., and Ridgwell, A., 2009, Ocean acidification in deep time: Oceanography, v. 22, p. 94–107.

Kuroyanagi, A., Kawahata, H., Suzuki, A., Fujita, K., and Takahiro, I., 2009, Impacts of ocean acidification on large benthic foraminifers: Results from laboratory experiments: Marine Micropaleontology, v. 73, p. 190–195.

Lee, J. J., 2006, Algal symbiosis in larger foraminifera: Symbiosis, v. 42, p. 63–75.

Macintyre, I. G., and Reid, R. P., 1998, Recrystallization in living porcelaneous foraminifera (*Archaias angulatus*): textural changes without mineralogic alteration: Journal of Sedimentary Research, v. 68, p. 11–19.

Martin, R. E., 1986, Habitat and distribution of the foraminifer *Archaias angulatus* (Fichtel and Moll) (Miliolina, Soritidae), northern Florida Keys: Journal of Foraminiferal Research, v. 16, p. 201–206.

Martin, S., Rodolfo-Metalpa, R., Ransome, E., Rowley, S., Buia, M.-C., Gattuso, J.-P., and Hall-Spencer, J., 2008, Effects of naturally acidified seawater on seagrass calcareous epibionts: Biology Letters, v. 4, p. 689–692.

McCloskey, B. J., 2009, Foraminiferal responses to arsenic in a shallow-water hydrothermal vent system in Papua New Guinea and in the laboratory: University of South Florida Graduate School Theses and Dissertations, http://scholarcommons.usf.edu/etd/2091.

McIntyre-Wressnig, A., Bernhard, J. M., McCorkle, D. C., and Hallock, P., 2013, Non-lethal effects of ocean acidification on the symbiont-bearing benthic foraminifer *Amphistegina gibbosa*: Marine Ecology Progress Series, v. 472, p. 45–60.

McIntyre-Wressnig, A., Bernhard, J. M., Wit, J. C., and McCorkle, D. C., 2014, Ocean acidification not likely to affect the survival and fitness of two temperate benthic foraminiferal species: results from culture experiments: Journal of Foraminiferal Research, v. 44, p. 341–351.

Meyer-Dombard, D. R., Amend, J., and Osburn, M. R., 2013, Microbial diversity and potential for arsenic and iron biogeochemical cycling in an arsenic-rich, shallow-sea hydrothermal vent (Tutum Bay, Papua New Guinea): Chemical Geology, v. 348, p. 37–47.

Meyer-Dombard, D. R., Price, R. E., Pichler, T., and Amend, J. P., 2012, Prokaryotic populations in arsenic-rich shallow-sea hydrothermal sediments of Ambitle Island, Papua New Guinea: Geomicrobiology Journal, v. 29, p. 1–17.

Morse, J. W., and Mackenzie, F. T., 1990, Geochemistry of Sedimentary Carbonates: Elsevier, Amsterdam, 707 p.

Nehrke, G., Keul, N., Langer, G., de Nooijer, L. J., Bijma, J., and Meibom, A., 2013, A new model for biomineralization and trace-element signatures of Foraminifera tests: Biogeosciences, v. 10, p. 6759–6767.

Newell, N. D., 1962, Paleontological gaps and geochronology: Journal of Paleontology, v. 36, p. 592–610.

Newell, N. D., 1982, Mass extinctions: illusions or realities?: Geological Society of America, Special Paper, v. 89, p. 63–91.

Pettit, L. R., Hart, M. B., Medina-Sánchez, A. N., Smart, C. W., Rodolfo-Metalpa, R., Hall-Spencer, J. M., and Prol-Ledesma, R. M., 2013, Benthic foraminifera show some resilience to ocean acidification in the northern Gulf of California, Mexico: Marine Pollution Bulletin, v. 73, p. 452–462.

Pichler, T., 2005, Application of stable and radiogenic isotopes as tracers for the origin, mixing and subsurface history of fluids in shallow-water hydrothermal systems: Journal of Volcanology and Geothermal Research, v. 139, p. 211–226.

Pichler, T., and Dix, G. R., 1996, Hydrothermal venting within a coral reef ecosystem, Ambitle Island, Papua New Guinea: Geology, v. 24, p. 435–438.

Pichler, T., and Veizer, J., 1999, Precipitation of Fe(III) oxyhydroxide deposits from shallow-water hydrothermal fluids in Tutum Bay, Ambitle Island, Papua New Guinea: Chemical Geology, v. 162, p. 15–31.

Pichler, T., and Veizer, J., 2004, The precipitation of aragonite from shallow-water hydrothermal fluids in a coral reef, Tutum Bay, Ambitle Island, Papua New Guinea: Chemical Geology, v. 207, p. 31–45.

Pichler, T., Veizer, J., and Hall, G. E. M., 1999a, The chemical composition of shallow-water hydrothermal fluids in Tutum Bay, Ambitle Island, Papua New Guinea and their effect on ambient seawater: Marine Chemistry, v. 64, p. 229–252.

Pichler, T., Veizer, J., and Hall, G. E. M., 1999b, Natural input of arsenic into a coral-reef ecosystem by hydrothermal fluids and its removal by Fe(III) oxyhydroxides: Environmental Science and Technology, v. 33, p. 1373–1378.

Pichler, T., Amend, J. P., Garey, J., Hallock, P., Hsia, N. P., Karlen, D. J., Meyer-Dombard, D. R., McCloskey, B. J., and Price, R. E., 2006, A natural laboratory to study arsenic geobiocomplexity: Eos, Transactions American Geophysical Union, v. 87, p. 221–225.

Prazeres, M. de Freitas, Martins, S., and Bianchini, A., 2011, Biomarkers response to zinc exposure in the symbiont-bearing foraminifer *Amphistegina lessonii* (Amphisteginidae, Foraminifera): Journal of Experimental Marine Biology and Ecology, v. 407, p. 116–121.

Prazeres, M. de Freitas, Martins, S., and Bianchini, A., 2012, Assessment of water quality in coastal waters of Fernando de Noronha, Brazil: Biomarker analysis in *Amphistegina lessonii*: Journal of Foraminiferal Research, v. 42, p. 56–65.

Price, R. E., 2008, Biogeochemical cycling of arsenic in the marine shallow-water hydrothermal system of Tutum Bay, Ambitle Island, Papua New Guinea: University of South Florida Graduate School Theses and Dissertations, http://scholarcommons.usf.edu/etd/460.

Price, R. E., and Pichler, T., 2005, Distribution, speciation and bioavailability of arsenic in a shallow-water submarine hydrothermal system, Tutum Bay, Ambitle Island, PNG: Chemical Geology, v. 224, p. 122–135.

Price, R. E., Amend, J., and Pichler, T., 2007, Enhanced geochemical gradients in a marine shallow-water hydrothermal system: unusual arsenic speciation in horizontal and vertical pore water profiles: Applied Geochemistry, v. 22, p. 2595–2605.

Price, R. E., London, J., Wallschläger, D., Ruiz-Chancho, M. J., and Pichler, T., 2013, Enhanced bioaccumulation and biotransformation of As in coral reef organisms surrounding a marine shallow-water hydrothermal vent system: Chemical Geology, v. 348, p. 48–55.

Raja, R., and Saraswati, P. K., 2007, A field-based study on variation in Mg/Ca and Sr/Ca in larger benthic foraminifera: Geochemistry, Geophysics, Geosystems, v. 8, Q10012.

Reymond, C. E., Lloyd, A., Kline, D. I., Dove, S. G., and Pandolfi, J. M., 2013, Decline in growth of foraminifer *Marginopora rossi* under eutrophication and ocean acidification scenarios: Global Change Biology, v. 19, p. 291–302.

Ries, J. B., Cohen, A. L., and McCorkle, D. C., 2009, Marine calcifiers exhibit mixed responses to CO_2-induced ocean acidification: Geology, v. 37, p. 1131–1134.

Rodolfo-Metalpa, R., Lombardi, C., Cocito, S., Hall-Spencer, J. M., and Gambi, M. C., 2010, Effects of ocean acidification and high temperatures on the bryozoan *Myriapora truncata* at natural CO_2 vents: Marine Ecology, v. 31, p. 447–456.

Russell, B. D., Connell, S. D., Uthicke, S., Muehllehner, N., Fabricius, K. E., and Hall-Spencer, J. M., 2013, Future seagrass beds: Can increased productivity lead to increased carbon storage?: Marine Pollution Bulletin, v. 73, p. 463–469.

Saxon, E., 2008, Noah's Parks: a partial antidote to the Anthropocene extinction event: Biodiversity, v. 9, p. 5–10.

Schmidt, C., Heinz, P., Kucera, M., and Uthicke, S., 2011, Temperature-induced stress leads to bleaching in larger benthic foraminifera hosting endosymbiotic diatoms: Limnology and Oceanography, v. 56, p. 1587–1602.

Segev, E., and Erez, J., 2006, Effect of Mg/Ca ratio in seawater on shell composition in shallow benthic foraminifera: Geochemistry, Geophysics, Geosystems, v. 7, Q02P09.

Sinutok, S., Hill, R., Doblin, M. A., Wuhrer, R., and Ralph, P. J., 2011, Warmer more acidic conditions cause decreased productivity and calcification in subtropical coral reef sediment-dwelling calcifiers: Limnology and Oceanography, v. 56, p. 1200–1212.

Souder, H. C., McCloskey, B. J., Hallock, P., and Byrne, R., 2010, Shell anomalies observed in a population of *Archaias angulatus* (Foraminifera) from the Florida Keys (USA) sampled in 1982–83 and 2006–07: Marine Micropaleontology, v. 77, p. 71–81.

Talge, H. K., and Hallock, P., 2003, Ultrastructural responses to bleaching in *Amphistegina gibbosa* (Foraminifera): Journal of Eukaryotic Microbiology, v. 50, p. 324–333.

Tans, P., and Keeling, R., 2013, Trends in atmospheric carbon dioxide, full Mauna Loa CO_2 record: http://www.esrl.noaa.gov/gmd/ccgg/trends.

Uthicke, S., Momigliano, P., and Fabricius, K. E., 2013, High risk of extinction of benthic foraminifera in this century due to ocean acidification: Scientific Reports, v. 3, article 1769.

Vogel, N., and Uthicke, S., 2012, Calcification and photobiology in symbiont-bearing benthic foraminifera and responses to a high CO_2 environment: Journal of Experimental Marine Biology and Ecology, v. 424–425, p. 15–24.

Zohary, T., Reiss, Z., and Hottinger, L., 1980, Population dynamics of *Amphisorus hemprichii* (Foraminifera) in the Gulf of Elat (Aqaba), Red Sea: Eclogae Geologicae Helvetiae, v. 73, p. 1071–1094.

Received 6 June 2014
Accepted 18 December 2014